

Scaling properties of a low-actuation pressure microfluidic valve

Vincent Studer and Giao Hang

Department of Applied Physics, California Institute of Technology, Pasadena, California 91125

Anna Pandolfi

Dipartimento di Ingegneria Strutturale, Politecnico di Milano, Milano, 20133, Italy

Michael Ortiz

Graduate Aeronautical Laboratories, California Institute of Technology Pasadena, California 91125

W. French Anderson

*Department of Applied Physics, California Institute of Technology, Pasadena, California 91125
and Gene Therapy Laboratories, Keck School of Medicine, University of Southern California,
Los Angeles, California 90033*

Stephen R. Quake^{a)}

Department of Applied Physics, California Institute of Technology, Pasadena, California 91125

(Received 16 June 2003; accepted 7 October 2003)

Using basic physical arguments, we present a design and method for the fabrication of microfluidic valves using multilayer soft lithography. These on-off valves have extremely low actuation pressures and can be used to fabricate active functions, such as pumps and mixers in integrated microfluidic chips. We characterized the performance of the valves by measuring both the actuation pressure and flow resistance over a wide range of design parameters, and compared them to both finite element simulations and alternative valve geometries. © 2004 American Institute of Physics.

[DOI: 10.1063/1.1629781]

INTRODUCTION

Understanding the physics of solid state devices such as diodes and transistors was a crucial enabling factor of the integrated circuit revolution. Semiconductor physics allowed the design of transistors with highly engineered performance properties, including speed, power consumption, size, gain, noise, breakdown current, and breakdown voltage. Microfluidic devices are now poised to use similar technology and ideas to launch a similar revolution in biology and the life sciences. For these integrated microfluidic circuits, the fundamental components will be valves, pumps, and other tools for fluidic manipulation. Working out the connection between the basic physics of the valves and their performance will be a key step in the development of a theory of “device physics” for these technologies. Some of the analogous performance criteria in fluidic devices are size, dead volume, channel dimensions, actuation pressure, and scalability.

The importance of the performance criteria depends on the application. For electrophoretic separation applications, there is a large body of literature showing how electrokinetic fluid manipulation can be used to meter and inject small amounts of fluid into separation columns. However, these methods are not general because they are highly dependent on the particular properties of the working fluid and are challenging to implement when there are complex plumbing requirements. A more general fluid manipulation solution is to use a mechanical valve, and there are many examples of microfabricated mechanical valves.¹ We have shown how to

fabricate integrated mechanical valves in monolithic elastomeric chips,² and that these valves can be used to make highly integrated chips that are roughly equivalent in their complexity to electronic integrated circuits fabricated with large scale integration.³ They also can be used in robust manipulation schemes that meter and mix independent of the properties of the working fluid.⁴

These elastomeric valves have proven to be valuable in applications involving bacterial cells and solution biochemistry. However, the physical properties of the valves do not scale well in the sense that the actuation pressures scale poorly as the channel dimensions vary, and achieving practical actuation pressures requires low aspect ratio geometry (~1:10). For many applications of interest it would be desirable to have unity aspect ratio channels and a greater dynamic range in the available dimensions. These criteria are particularly important for the design of high density chips to manipulate eukaryotic cells. Here, we describe a type of microfluidic valve with extremely low actuation pressures and favorable scaling properties. We characterized the performance of the valves by measuring both the actuation pressure and flow resistance over a wide range of design parameters, including unity aspect ratio channels. We found close agreement between the measured data and finite element simulations, thus validating the simulations as a design tool for future microfluidic device design.

SCALING AND DESIGN PRINCIPLES

Most mechanical valve schemes involve the use of a deflectable membrane that closes off a fluid channel or chamber. In order to have high density devices, it is desirable

^{a)}Electronic mail: quake@caltech.edu

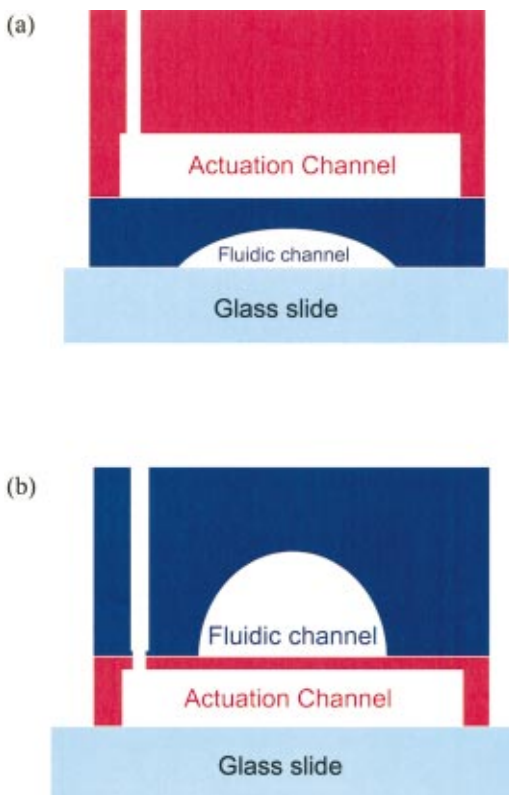


FIG. 1. (Color) (a) Schematic diagram of a push-down valve geometry, in which a curved membrane of variable thickness is deflected to close off a fluidic channel when pressure is applied to the actuation channel. This type of geometry requires a large aspect ratio in the dimensions of the fluidic channel. (b) Schematic diagram of a push-up valve geometry, in which a membrane of uniform thickness is deflected to close a rounded fluidic channel when pressure is applied to the actuation channel. This geometry allows extra design flexibility because the thickness of the membrane is decoupled from the dimensions of the fluidic channel. In both cases, flow in the fluidic channel is perpendicular to the page; flow in the actuation channel is parallel to the page (figure not to scale).

to minimize the size of a membrane valve while simultaneously minimizing the actuation pressure of each valve. Geometry plays an obvious role in this, as do the material properties of the membrane. Silicone elastomers such as polydimethylsiloxane (PDMS) have Young's moduli that are five orders of magnitude smaller than hard materials such as silicon and silicon nitride, thus allowing lower actuation pressures than are found in microelectromechanical systems type valves. Furthermore, it is desirable to use a deformable material such as PDMS as a gasket to ensure leak-proof operation, just as macroscopic valves use rubber washers as valve seats.

Figure 1 shows schematic diagrams of two valve geometries. Part (a) shows the geometry used in our previous work, called "push-down" because the membrane between the channels is pushed down to seal off the lower channel, which contains the fluid of interest. The thickness of the membrane varies from the edge of the channel to the middle. This geometry has proven useful in a number of applications and has the advantage that the lower fluid channel can be sealed against any substrate of interest, meaning that fluidic devices can be used as removable print heads on solid substrates, and that devices can be easily removed from a sub-

strate and cleaned for reuse. Part (b) shows the low actuation pressure geometry that we refer to as "push-up," because the membrane deflects upwards to seal off the upper fluid channel. In this geometry, the deflectable membrane is uniform and featureless. There have been previous demonstrations of similar geometries in hybrid devices, where a featureless PDMS membrane is sandwiched between two patterned, hard substrates;⁵⁻⁷ however, these have tended to be large (millimeter dimensions) and rather slow. Here we have shown how to fabricate such valves with $100\ \mu\text{m}$ dimensions into monolithic PDMS chips and have made an extensive characterization of valve performance. The push-up geometry is advantageous because the uniformity and independent nature of the membrane thickness simplifies the dependence of the actuation pressure on the depth of the fluid channel.

DEVICE FABRICATION

In order to fabricate high aspect ratio fluidic channels, we spin coated a thick positive photoresist (AZ 100 XT PLP) on a 3 in. silicon wafer and patterned it by standard photolithography. Once developed, the photoresist was heated above its glass transition temperature (typically at $140\ ^\circ\text{C}$ for 5 min), thus allowing reflowing of the photoresist in order to obtain channels with a rounded cross section. Molds for the actuation channels were made out of SU-8 50, an epoxy based negative photoresist. This photoresist does not reflow at the temperatures required for the curing of the elastomer, and SU-8 lines keep their rectangular cross section.⁸ The SU-8 was spin coated at 2000 rpm for 1 min on a 3 in. silicon wafer. The thickness of the SU-8 layer was typically $50\ \mu\text{m}$.

Both molds were then exposed to a vapor of trimethylchlorosilane for 1 min in order to facilitate mold release. Then the two component silicone elastomer (GE RTV 615) was poured on the fluidic channel mold placed in a plastic petri dish; the elastomer was also spun onto the actuation channel mold. The fluidic channel layer has an excess in curing agent (GE RTV 615 B) whereas the actuation channel layer has an excess in the other component (GE RTV 615 A), as described previously² thus allowing further bonding between the two cured layers. The thickness of the actuation channel layer is controlled by the spin coating speed. This parameter is highly relevant since it controls the thickness of the active membrane. The fluid channel layer is several millimeters thick to allow reliable connections with macroscopic elements such as tubing and syringes.

Both layers are cured in an oven for 45 min at $80\ ^\circ\text{C}$. Then the fluidic channel layer is peeled off from the mold. Access holes to the fluid channels are punched using a clean luer stub adapter. This layer is then trimmed, cleaned with ethanol, dried with nitrogen and optically aligned to the actuation channel layer. Bonding between the two layers is achieved by baking at $80\ ^\circ\text{C}$ for 3 h. The assembled chip is peeled from the actuation channel mold and access holes to the actuation channels are punched. The final device is then sealed to a precleaned glass microscope slide by rinsing both surfaces (glass and RTV) with ethanol, drying with nitrogen and baking for 3 h at $80\ ^\circ\text{C}$. With clean surfaces, pressures up

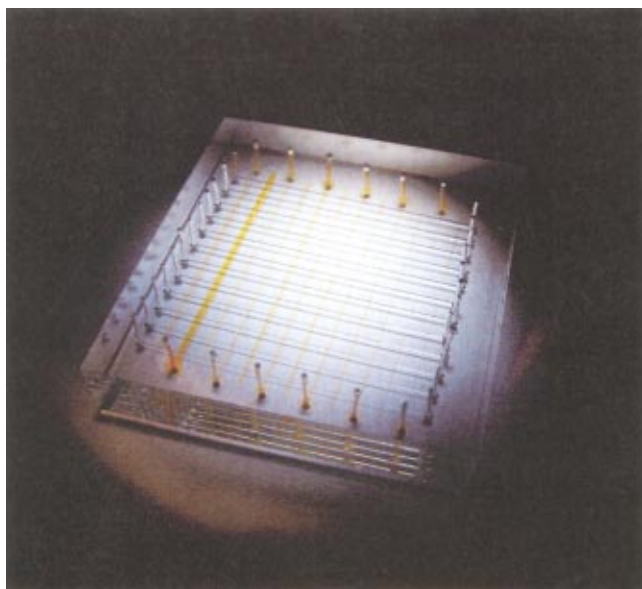


FIG. 2. (Color) Photograph of a valve matrix chip. The chip is a 12×12 array of fluidic and actuation channels which form a matrix of 144 valves whose membrane dimensions vary according to the dimensions of the channels. The actuation channels are filled with an orange dye solution. Chip is $1'' \times 1''$.

to 30 psi can be applied to the actuation channels without leakage.

EXPERIMENTS

In order to measure the performance of the microfluidic valve design, different devices were constructed. One device was constituted of 12 parallel fluidic channels with width from 50 to $600 \mu\text{m}$, crossed by 12 actuation channels with the same width range (Fig. 2). Using these devices, we studied the variations of the actuation pressure (pressure at which the fluidic channel is completely closed by the valve) with the width of the fluid channels and the width of the actuation lines. We also made different devices with different spin coating speeds of the actuation channel layer in order to characterize the dependence of the actuation pressure on the membrane thickness.

The elastomer is permeable to gas, so that by applying pressure on the actuation channel one can create a flow of air from the actuation channel into the surrounding elastomer. Since this process can create air bubbles in the fluid channels, the actuation channels are filled with a colored solution of orange G in de-ionized water to minimize the volume of air that passes through the membrane. The dye is pushed into the actuation channel, squeezing a small volume of air out of the channel. Actuation pressures were measured with the fluid channel empty. The large index change makes it straightforward to image the closure of the valve when the membrane comes into contact with the top of the fluid channel. When there is liquid in the fluid channel, the actuation pressure is shifted by the backpressure of the liquid. Once the actuation pressures were measured, chips were cut along the actuation channels, and the membrane thicknesses were measured by using an optical microscope with a $100\times$ objective lens.

Another device was designed to measure the pressure drop induced by one valve as a function of the pressure in the actuation channel, using a method of compensated *in situ* measurement.⁹ This device has a Y-shaped fluidic channel. One side is connected to a reservoir filled with de-ionized water and has a valve next to the inlet; the other side is connected to a reservoir filled with a solution of 100 nm diameter fluorescent beads (Duke Scientific Corp. R100) in de-ionized water and has no valve. The position of the interface between the two solutions was plotted against the difference of hydrostatic pressure between the two branches of the fluidic channel (only the reservoir with beads is moved). Then, with no pressure difference between the two branches, the position of the interface was measured for different values of the pressure on the actuation channel. We then used the previous calibration plot to interpolate the value of the corresponding resistance induced by the valve.

NUMERICAL SIMULATIONS

In order to gain insight into the experimental data, we have developed a full three-dimensional, finite-deformation model of a single microvalve. By way of validation, we present a suite of numerical tests which demonstrates the fidelity of the model as regards sensitive predictions of microvalve behavior, such as the dependence of the actuation pressure on the geometry of the valve. The validated model provides a powerful basis for the rational design of high-performance microvalves, including gain, bistability, and other advanced features.

The elastomer is modeled as a near-incompressible Neo-Hookean material, a constitutive model which describes the behavior of rubber-like materials undergoing large deformations.¹⁰ The Neo-Hookean model has some basis in theory: it is obtained by a statistical-mechanical treatment of the deformations of freely jointed molecular chains. From this analysis one obtains the relation $\mu = NkT$, where μ is the ground-state shear modulus, T is the absolute temperature, k is the Boltzmann constant, and N is the number of chains per unit volume. The material behavior then is characterized by two parameters: the shear modulus μ and Poisson's ratio ν of the undeformed configuration. In calculations we use $\mu = 0.6 \text{ MPa}$ and $\nu = 0.45$; both are well accepted in the literature.¹⁰

We resort to the finite element method in order to represent the three-dimensional geometry of the microvalves and to solve the equations governing their deformation and closure. The elements employed in the calculations are ten-node quadratic tetrahedral with four gauss points (Fig. 6). A uniform pressure is applied over the surface of the actuation channel. Frictionless contact is enforced between all surfaces by a nonsmooth contact algorithm.¹¹ The resulting equilibrium configuration of the microvalve is computed by dynamic relaxation.¹² Owing to the twofold symmetry of the problem, the computational model is restricted to 1/4 of the microvalve, with symmetry boundary conditions applied on all symmetry planes. For each microvalve geometry, the pressure is increased monotonically at 1/10 increments of the experimental actuation pressure, and the largest pressure not

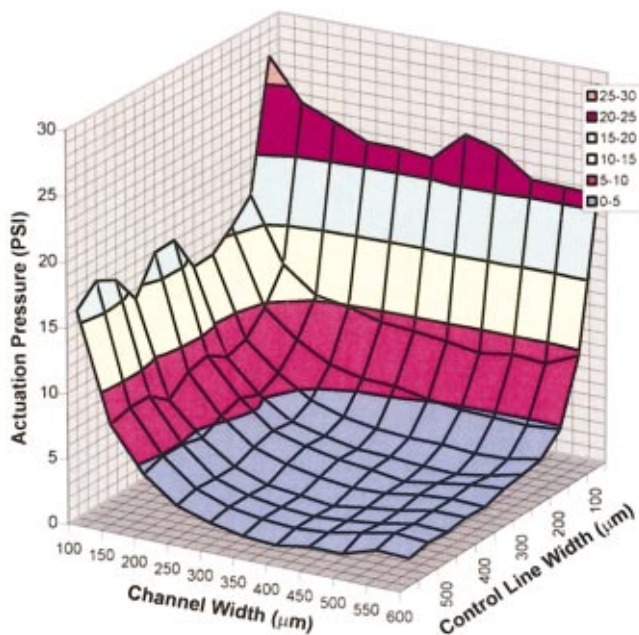


FIG. 3. (Color) Actuation pressures of valves from the matrix chip. The actuation pressures are symmetric with channel widths and significantly smaller than the pressures required to actuate push-down valves with comparable dimensions.

resulting in full closure of the microvalve is recorded as the actuation pressure.

A parametric study concerns the effect of membrane thickness on the actuation pressure. The actuation channel section is rectangular, at a width of $300\ \mu\text{m}$ and a height of $56\ \mu\text{m}$, and the fluidic channel section is bounded by a circular arc $300\ \mu\text{m}$ in width and $50\ \mu\text{m}$ in height. Three membrane thicknesses in the experimental range, 5, 10, and $15\ \mu\text{m}$, are considered. Another parametric study concerns the effect of channel width on actuation pressure. In this case, the actuation channel section is rectangular, $100\text{--}600\ \mu\text{m}$ in width and $55\ \mu\text{m}$ in height, and the fluidic channel section is bounded by a circular arc $228\ \mu\text{m}$ in width and $54\ \mu\text{m}$ in height. The calculations are carried out for four actuation channel widths, 200, 300, 450, and $550\ \mu\text{m}$, in the experimental range.

RESULTS

We mapped the actuation pressure of the push-up valve structure as a function of the three parameters that characterize the membrane—width, length, and thickness. As expected, the results are symmetric as a function of the width and thickness (Fig. 3), with larger dimensions yielding smaller pressures. As the width of the actuation channel becomes small relative to the fluidic channel width, the actuation pressure begins to scale roughly as the inverse power of width or length. (Fig. 4, bottom). For small actuation channel width, the actuation pressure increases dramatically. As the actuation channel becomes wider than an optimum value, the actuation pressure stays steady. It is therefore possible to have actuation channels crossing fluidic channel by reducing their

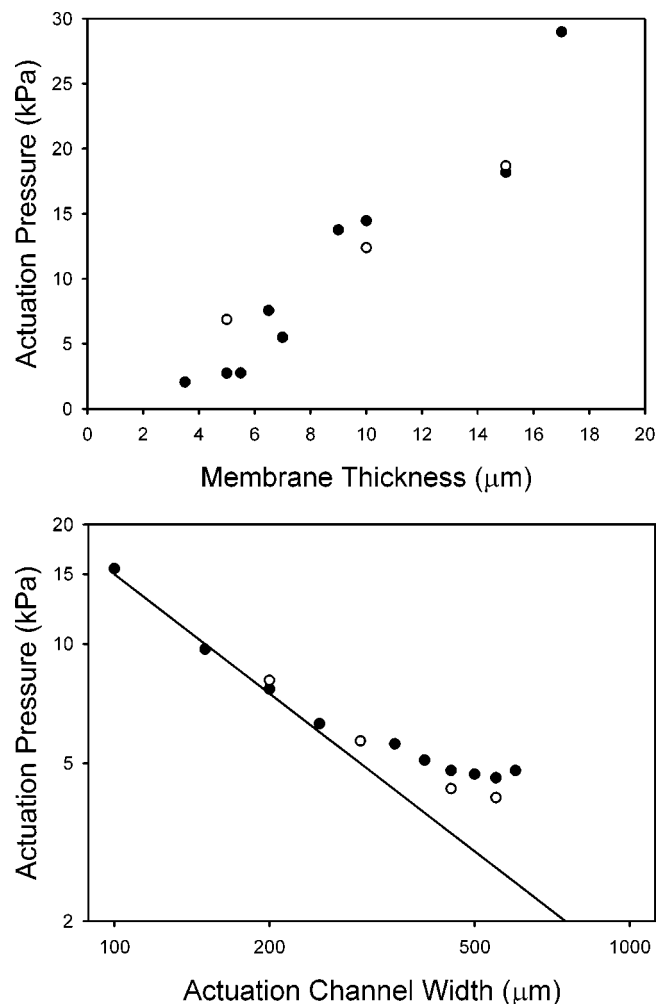


FIG. 4. Top: actuation pressure as a function of membrane thickness for a valve with a $300\ \mu\text{m}$ actuation channel and $300\ \mu\text{m}$ fluidic channel. Closed symbols represent measured valves; open symbols represent values calculated by finite element simulation. Bottom: a subset of the data from Fig. 3 shows the scaling of actuation pressure with membrane dimensions as actuation channels of various dimensions close valves over a fluidic channel that is roughly $228\ \mu\text{m}$ in width and $54\ \mu\text{m}$ in height. The line has slope -1 .

width at the crossing points. This allows the creation of complex chip designs and multiplexers³ in order to control multiple valves with one actuation channel.

The actuation pressure also scales with the membrane thickness. Figure 4, top, shows the variation of the actuation pressure with the membrane thickness for a $300\ \mu\text{m}$ wide actuation line and a $300\ \mu\text{m}$ wide fluidic channel. The fluidic channel is $56\ \mu\text{m}$ deep, and the cross section is close to an arc. Although the results show that the actuation pressure appears to increase linearly with the membrane thickness, the nonzero offset implies that the true functional dependence is more complicated.

In both cases, the agreement with the simulations is excellent. Figure 4, top, shows a comparison of measured (closed circles) and calculated (open circles) actuation pressures. The predicted values closely match the experimental data, which provides a validation of the model. Figure 5, bottom, also compares the predicted and measured actuation pressures as a function of channel width. Again, the predictions of the model are consistent with observation, with the

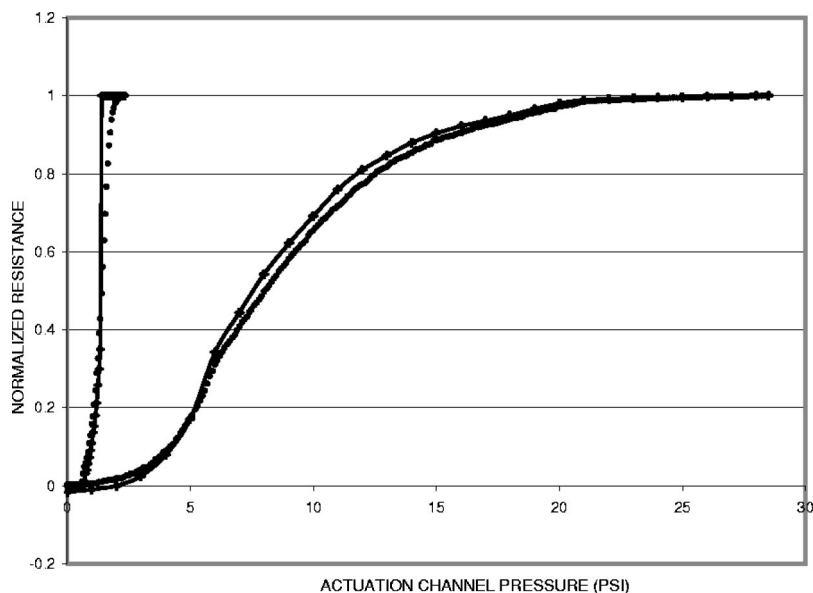


FIG. 5. Performance comparison of push-up (left) and push-down (right) valves of identical dimensions. By making a differential measurement of the extra resistance provided in a channel by the valve, it is possible to map out the effective resistance of the valves as a function of applied pressure. Thus, it is clear that the push-up valve actuates at a pressure about an order of magnitude lower than the push-down valve. Push-up valves show hysteretic behavior due to the membrane sticking to the opposing channel.

actuation pressure slightly underpredicted (overpredicted) for large (small) actuation channel widths.

The thinnest membranes we were able to create were a few microns. For very thin membranes, surface tension effects due to the photoresist features on the wafer create an uneven surface. Thus, the membrane thickness, which is the difference between the thickness of the layer of elastomer and the thickness of the photoresist features, begins to vary with the pattern density, size, and shape. Moreover, these nonflat surfaces make the bonding between the layers of the device difficult to achieve because of residual air bubbles between the two layers.

We made a direct comparison of the performance of push-up and push-down valves with identical dimensions. In both cases the actuation channel was $300\ \mu\text{m}$ wide, while the fluid channel was $200\ \mu\text{m}$ wide and $46\ \mu\text{m}$ deep and the membrane was $10\ \mu\text{m}$ thick. The pressure on the input of the fluid channel was $490\ \text{mm}$ of H_2O , ($0.68\ \text{psi}$), while the output was at atmospheric pressure. A plot of the normalized resistance (fraction of the input pressure) of the valves as a function of the actuation channel pressure is shown in Fig. 5.

Both valves have similar shaped curves for increasing values of the pressure in the actuation channel. However, the curves are offset by a significant amount and the pressure at which the push-down valve closes is more than $20\ \text{psi}$, while the closing pressure for the push-up valve is only $2.4\ \text{psi}$. This difference of one order of magnitude is due to the shape difference of the active membrane. For the push-up valve, the membrane is uniformly thin. The push-down valve has a convex shaped membrane. It is thin in the center ($10\ \mu\text{m}$), but much thicker at the edges ($46\ \mu\text{m}$) and therefore harder to bend. In fact, for this type of valve, there is an optimum value of the membrane thickness. If the membrane is too thin, it deflects only in the center and the valve never closes on the edges. If the membrane is too thick and very stiff, the actuation pressure becomes impractically high and the device fails. For the push-up valve, there is only a technical limitation to the membrane thickness, since a thinner membrane

always gives a lower actuation pressure. Therefore, push-up valves are suitable for high aspect ratio channels. It is typically possible to close channels with aspect ratio higher than 5:1 (width:depth) with a pressure lower than $5\ \text{psi}$.

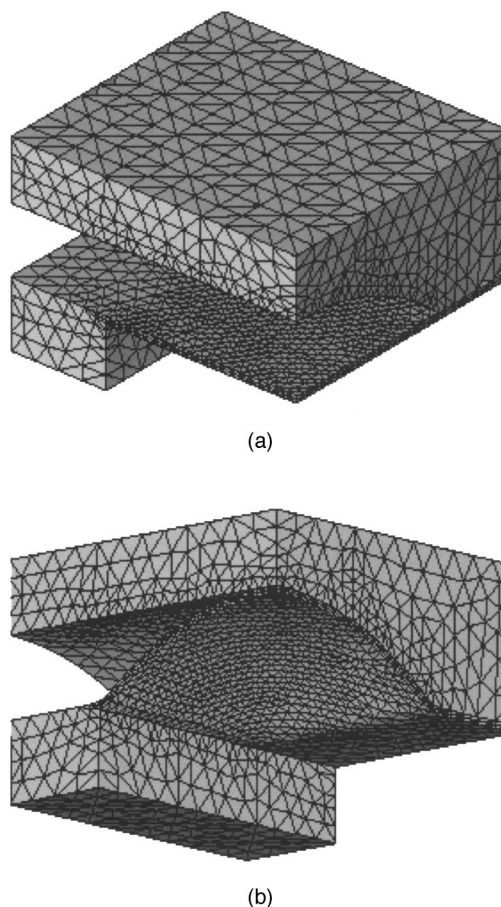


FIG. 6. Computational model of a microvalve consisting of a $300 \times 56\ \mu\text{m}$ control channel, a $300 \times 50\ \mu\text{m}$ fluidic channel, and a $5\text{-}\mu\text{m}$ -thick membrane. The mesh consists of 3365 nodes and 1622 ten node tetrahedral finite elements. (a) Undeformed configuration (b) Deformed configuration at actuation pressure.

For decreasing values of the pressure, the push-up valve shows an interesting hysteresis. Figure 5 shows that the channel resistance increases smoothly as the actuation pressure is increased. However, as the pressure is decreased, the resistance remains high, then takes a discontinuous jump downwards. We used an optical microscope with a long working distance objective to image the valve end on, and were able to capture the shape and position of the membrane for different values of the pressure in the actuation channel. This analysis showed that the hysteresis comes from the sticking of the membrane on the top of the fluidic channel. When the force on the membrane due to the pressure difference between the fluidic channel and the actuation channel overcomes the adhesion of the membrane to the top of the fluidic channel, the valve suddenly snaps open and the value of the pressure drop induced by the valve goes down to a value close to the one obtained for increasing pressures. This hysteresis was not observed for the push-down valve, probably because the larger restoring forces were able to overwhelm the surface forces of sticking.

CONCLUSIONS

We have shown that by using simple physical arguments it is possible to design, fabricate, and test monolithic microvalves with favorable scaling properties. These valves have an order of magnitude lower actuation pressures than the best previous design with similar dimensions. They have excellent scaling properties in the sense that they can be used to make unity-aspect ratio valves with a large dynamic range in

dimensions. The fact that simulations agree so well with the valve performance means that simulation can be used as a tool for future valve designs, in particular when making complex geometries, seeking to scale to ever smaller dimensions, or as a tool to elucidate the basic physics of valve closing.

- ¹See, e.g., S. Shoji, *Top. Curr. Chem.* **194**, 163 (1998); G. T. A. Kovacs, *Micromachined Transducers Sourcebook* (McGraw Hill, New York, 1998).
- ²M. Unger, H. P. Chou, T. Thorsen, A. Scherer, and S. Quake, *Science* **288**, 113 (2000).
- ³T. Thorsen, S. J. Maerkl, and S. R. Quake, *Science* **298**, 580 (2002).
- ⁴C. L. Hansen, E. Skordalakes, J. M. Berger, and S. R. Quake, *Proc. Nat'l. Acad. Sci. USA* **99**, 16531 (2002).
- ⁵C. Vieider, O. Ohman, and H. Elderstig, Technical Digest of the 8th International Conference on Solid State Sensors and Actuators, Stockholm, Sweden, June 25–29 1995, Vol. 2, pp. 284–286.
- ⁶X. Yang, C. Grosjean, Y. C. Tai, and M. Ho, *Sens. Actuators A* **64**, 101 (1998).
- ⁷W. H. Grover, A. M. Skelley, C. N. Liu, E. T. Lagally, and R. A. Matthies, *Sens. Actuators B* **89**, 315 (2003).
- ⁸V. Studer, A. Pepin, and Y. Chen, *Appl. Phys. Lett.* **80**, 3614 (2002).
- ⁹A. Groisman, M. E. Enzelberger, and S. R. Quake, *Science* **300**, 955 (2003).
- ¹⁰R. W. Ogden, *Mechanics of Solids* (Pergamon, New York, 1982), pp. 499–537.
- ¹¹C. Kane, E. A. Repetto, M. Ortiz, and J. E. Marsden, *Comput. Methods Appl. Mech. Eng.* **180**, 1 (1999); A. Pandolfi, C. Kane, J. E. Marsden, and M. Ortiz, *Int. J. Numer. Methods Eng.* **53**, 1801 (2002).
- ¹²P. Underwood, in *Computational Methods for Transient Dynamic Analysis*, edited by T. Belytschko and T. J. R. Hughes (Elsevier Science, Amsterdam, 1983), pp. 245–265; D. R. Oakley and N. F. Knight, Jr., *Comput. Methods Appl. Mech. Eng.* **126**, 67 (1995).